Limits of size scalability of diffusion and growth: Atoms versus molecules versus colloids

N. Kleppmann,[1] F. Schreiber,[2,*] and S. H. L. Klapp[1,†]

[1]*Institut für Theoretische Physik, Technische Universität Berlin, Hardenbergstraße 36, 10623 Berlin, Germany*
[2]*Institut für Angewandte Physik, Universität Tübingen, Auf der Morgenstelle 10, 72076 Tübingen, Germany*

Understanding fundamental growth processes is key to the control of nonequilibrium structure formation for a wide range of materials on all length scales, from atomic to molecular and even colloidal systems. While atomic systems are relatively well studied, molecular and colloidal growth are currently moving more into the focus. This poses the question to what extent growth laws are size scalable between different material systems. We study this question by analyzing the potential energy landscape and performing kinetic Monte Carlo simulations for three representative systems. While submonolayer (island) growth is found to be essentially scalable, we find marked differences when moving into the third (vertical) dimension.

Interfacial growth dynamics continues to be a focus of intense research, relating concepts of nonequilibrium (statistical) physics [1] to application-related areas such as the fabrication of epitaxial thin films [2], the formation of photonic crystals [3], the design of (hybrid) semiconductor devices [4,5], and the (directed) self-assembly of nano- and microscale particles into (crystalline) novel materials [6–10]. From the fundamental side, a major challenge is to understand and eventually *control* growth depending on a system's microscopic properties such as the type of interactions and the resulting surface kinetics [11]. In this regard, the best studied case, both experimentally (see, e.g., [12,13]) and theoretically [1,2,14–16], is that of atomic homoepitaxy. Inspired also by the strong current interest in organic and hybrid thin films, recent studies of growth focus more on molecular systems [4,17–22] and colloids [10,23] characterized by much larger length (nanometer to micrometer) and time scales. These developments raise intriguing questions: Can the detailed results established for atomic homoepitaxy be translated to molecular and colloidal systems? Is there a "size scalability" of growth phenomena? One might expect that for appropriate adjustment of the length, time, and possibly temperature scales, the resulting morphologies are similar. However, while recent work on colloidal epitaxy suggests that certain observables are indeed scalable (mostly for submonolayer growth) [23], the question on the *overall* scalability remains open.

The limitations of size scaling become apparent already in a simplified picture. The generally different pair interaction potentials $V(r)$ and, in particular, the different *attraction ranges* Δ of $V(r)$ (relative to the particle size σ) for atoms versus molecules versus colloids give rise to different diffusion barriers (see further below). Let us assume for simplicity that these enter the in-plane (i.e., intralayer) diffusion constant $D_\parallel$ via an effective energy barrier E_B in an Arrhenius-like manner, i.e., $\propto \exp(-E_B/k_B T)$, where k_B is Boltzmann's constant and T is the temperature. If this applies, then the in-plane diffusion rates of systems characterized by different length and time scales (atoms, molecules, and colloids) can be made

similar by simply adjusting the temperature. Considering the initial stages of growth, in the simplest picture (nucleation via stable dimers) the critical island density is expected to follow approximately $n_c \propto (D_\parallel/F)^{-1/3}$ where F is the adsorption rate (flux), produced in whatever form. This was indeed reported for the submonolayer regime over a remarkably large dynamic range [23]. It is tempting to assume that if we want a colloidal system to behave similar to an atomic system, then the temperature T^{colloid} of the colloidal system can be chosen such that the island density is similar to the atomic system (observed at some $T^{\mathrm{atom}} \neq T^{\mathrm{colloid}}$). Importantly, this would fix T^{colloid}. Going now beyond the initial stage (multilayer regime), the vertical distribution of material will be determined also by the effective out-of-plane (i.e., interlayer) diffusion constant $D_\perp$ related to the Ehrlich-Schwoebel barrier E_s [24,25]. Since generally E_s is of course different from E_B, this implies that for different E_s, the resulting $D_\perp$ is different, and so is the out-of-plane morphology. As a consequence, while *some* quantities such as n_c may follow remarkably well the concept of size scalability we expect the *overall* morphology (in-plane *and* out-of-plane distribution of material) to be generally *not* the same, i.e., not scalable.

In this Rapid Communication, we address the fundamental issue of the limitations of size scalability of growth morphologies, using analytical calculations and kinetic Monte Carlo (KMC) simulations. We first analyze in detail how different $V(r)$ (and, in particular, Δ) impact the different diffusion processes, by considering three homoepitaxial systems: atoms (with Ag as representative), the molecule C60, and colloids. To isolate the impact of Δ we focus on *spherical* systems, i.e., without explicit orientational degrees of freedom [17,26]. We then investigate the consequences of Δ on key observables quantifying the growth behavior, including the island density, the evolution of the individual layer coverages, and the shape (compactness) of the islands. We demonstrate the effect of Δ and the limits of size scalability.

Potential landscapes. Interactions between atoms typically extend over roughly one atomic diameter [27], which we consider long ranged. For colloids, the interactions can be tailored relatively well. In order to identify the impact of Δ, we here focus on colloids with short-ranged interactions with a range of only a few percent of the particle diameter. This case can be realized by depletion effects [28]. Finally, C60 has an
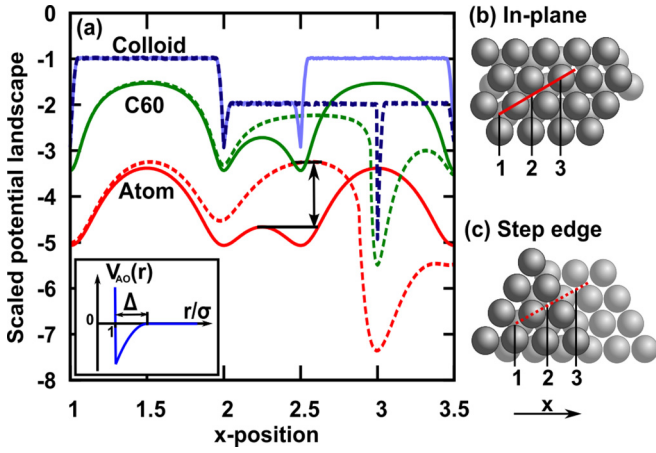
FIG. 1. Part (a) depicts potential landscapes sampled along the lines across a closed substrate layer, as well as across a step edge, as illustrated in parts (b) and (c). Solid lines denote in-plane sampling, while dashed lines denote sampling across a step edge. The pair potentials used in part (a) are the Lennard-Jones potential (atomic) [27], the Girifalco potential (C60) [29,30], and the Asakura-Oosawa potential [28] (see inset) with attraction range $\Delta = 0.05\sigma$ (colloidal). All pair potentials are scaled such that the well depth is -1 and the intersection with 0 is at 1 (defining the diameter σ). The double arrow in part (a) illustrates the barrier E_s that an atom has to overcome to cross the step edge. The units of the x axis are in-plane lattice constants.

(effective) interaction potential with a range in between those of atoms and colloids [18,29,30].

To understand the effect of Δ we first consider the energy landscape experienced by a tracer particle (Fig. 1). Substantiating earlier considerations by Ganapathy *et al.* [23], we here *quantify* these landscapes by using established potentials $V(r)$ for the three systems of choice. The resulting landscapes are effective in the sense that $V(r)$ already involves integrations over internal degrees of freedom (of the solvent in the case of colloids [28,31] or rotations in the case of C60 [29]) and thus, entropic effects. This is in contrast to approaches based on energy minimization with all degrees of freedom (see, e.g., [19]). For the atomic system [red lines in Fig. 1(a)] the resulting landscape displays soft mounds between energetically most favorable binding sites. The soft undulations reflect that the tracer always "feels" at least three neighbors due to the relatively large Δ. Further, the step-edge path is characterized by an energetic barrier significantly larger than those encountered for in-plane diffusion. The difference between the energy maximum at $x \approx 2.5$ and the corresponding in-plane diffusion barrier (see black double arrow) constitutes the step-edge barrier E_s [24,25].

The potential landscape of colloids (blue lines) is strikingly different. We note that this subject could easily be a longer study by itself. Indeed, the "potential landscape" of colloids typically has intrinsically entropic contributions due to the presence of a (fluctuating) solvent which influences both colloid-colloid and colloid-substrate interactions. These contributions depend on the specific system considered. Here we rather focus on our goal to identify the impact of Δ. To this end

we have chosen $V_{\text{colloid}}(r)$ such that the (depletion-induced) Δ is only 5% of the diameter, corresponding to the system considered in [23]. The resulting in-plane path displays a "dip" at position $x = 2.5$; however, due to the small Δ this dip is essentially delta-like. The step-edge path is characterized (between $2 < x < 3$) by a *constant* energy which matches the corresponding in-plane value. Thus, the *energetic* step-edge barrier entirely vanishes, and one is left with a "geometric" step-edge barrier generated solely by the different *lengths* of diffusion paths.

The C60 system is intermediate with respect to both the sharpness of the landscape variations (see Fig. 1) and the character of the step-edge barrier [18]. Thus, the colloidal landscape represents the limiting case for ultrashort attraction. This observation is in line with recent studies on the free energy landscape related to colloidal cluster formation, which is purely defined by geometry if $\Delta \to 0$ [32]. Using simple geometric considerations we have determined (for hard-core particles on a hexagonal lattice) the critical attraction range, Δ_c, beyond which the step-edge barrier becomes energetic: The criterion is whether the diffusing particle "feels" all three neighbors at all times (as is the case for atoms). From this we find $\Delta_c = \sqrt{3/2} - 1 \approx 0.225$. For $\Delta > \Delta_c$, the free diffusion barrier is lowered with respect to the step-edge barrier, yielding an E_s of energetic origin.

Towards the third dimension. These fundamental differences concerning step-edge diffusion are expected to strongly influence the growth behavior. To explore these effects quantitatively, we now consider hopping rates determining the dynamics of the systems in the framework of a (lattice-based) KMC approach [18,22,33,34]. For atomic and molecular systems (consisting of roughly spherical molecules), hopping between lattice sites i and j is commonly described using an Arrhenius-like rate. Here we employ the Clarke-Vvedensky bond-counting *ansatz* [35], which has been used in a variety of recent atomic [33,36,37] and C60 growth studies [18,22],

$$r_{i,j}^{\text{atoms/molecules}} = \nu_0 \exp\left(-\frac{E_{\text{free}} + n_i E_n + s_{i,j} E_s}{k_B T}\right), \quad (1)$$

where ν_0 is the attempt frequency, E_{free} denotes the barrier for diffusion of a free particle, n_i is the number of lateral (nearest) neighbors, and E_n is the bond strength to each neighbor. Finally, $s_{i,j} = 1$ if the diffusion path leads across a step edge and 0 otherwise. Within this model, the in-plane diffusion constant $D_\parallel$ (during island nucleation) is related to the free diffusion and binding contributions, i.e., $D_\parallel \propto \exp(-E_B/k_B T)$ with $E_B = E_{\text{free}} + n_i E_n$ [36], while the out-of-plane diffusion constant $D_\perp$ is related to the total barrier $E_\perp = E_{\text{free}} + n_i E_n + E_s$ (after appropriate averaging). Importantly, Eq. (1) has been shown to reproduce established scaling laws for atoms such as the dependence of the critical island size on the ratio $D_\parallel/F$ [36].

As discussed above, typical colloids with small Δ do not experience an energetic step-edge barrier E_s. Instead, E_s is determined by the ratio of path lengths for in-plane and out-of-plane diffusion. Thus, it would appear counterintuitive to model the impact of E_s by a simple Arrhenius behavior, as is done in Eq. (1). We thus propose a different model (which, however, does not impact our general conclusions).

According to experiments [23], the residence time of a colloid at a site touching three particles scales linearly with the diffusion path length. As the step-edge diffusion path is d times longer than the in-plane path, the waiting time associated with a step-edge diffusion process is also larger by a factor d. Thus, the rate [which corresponds to an inverse (average) time] is reduced by a factor d. Based on these considerations, we make the following *ansatz* for the hopping rate of colloids (with short-ranged interactions such as those in Fig. 1):

$$r_{i,j}^{\text{colloids}} = \frac{\nu_0}{1 + s_{i,j}(d-1)} \exp\left(-\frac{E_{\text{free}} + n_i E_{\text{n}}}{k_{\text{B}}T}\right). \quad (2)$$

For $s_{i,j} = 0$ (in-plane), $r_{i,j}^{\text{colloids}}$ is identical to the corresponding expression for atoms/molecules in Eq. (1), while for $s_{i,j} = 1$ (step-edge crossing), it reflects the reduction by a factor d. The latter is a *temperature-independent* effect. Note that one can formally rewrite the prefactor $1/d$ as $\exp(-G/k_{\text{B}}T)$ with $G = -k_{\text{B}}T \ln(1/d)$. Thus, when considering one temperature, Eq. (2) is comparable with Eq. (1), but with a "Schwoebel barrier" G of entropic nature (linear in $k_{\text{B}}T$) [31].

We now turn to the growth behavior. To this end we have performed KMC simulations based on Eqs. (1) and (2) at one flux rate ($F \approx 1$ ML min^{-1}).

Regarding the energy parameters, we set $E_{\text{free}} = 0.54$ eV in accordance with our previous studies for C60 [18,22]. We use this value for all three systems to obtain some degree of comparability (this corresponds to scaling F suitably). Due to the effective nature of the potential landscapes in Fig. 1(a), a precise quantification of E_{n}, even though it obviously depends on the material system. Following previous studies we set $E_{\text{n}}^{\text{C60}} = 0.13$ eV [18] and $E_{\text{n}}^{\text{atom}} = 0.72$ eV [22]. For typical colloids, the pair interactions are tunable by changing solvent parameters, thus, there is not one unique choice for $E_{\text{n}}^{\text{colloid}}$. Here we choose $E_{\text{n}}^{\text{colloid}} = 0.1$ eV, yielding $E_{\text{n}}^{\text{colloid}} < E_{\text{n}}^{\text{C60}} < E_{\text{n}}^{\text{atom}}$. This sequence reflects that the attraction range of the colloidal interaction potential is the smallest among the three systems considered. Regarding the step-edge diffusion, earlier studies suggest that there is only little energetic difference in magnitude between the Ehrlich-Schwoebel barrier of atoms and C60 [22]. Correspondingly, we set $E_{\text{s}}^{\text{atom}} = E_{\text{s}}^{\text{C60}} = 0.11$ eV. We have explicitly tested that the specific choice of energy parameters does not affect our general conclusions.

For the simulated colloidal systems the parameter d [see Eq. (2)], which corresponds to the ratio of path lengths of step-edge and in-plane diffusion, takes over the function of a step-edge barrier. Here we use a coarse-grained (triangular) lattice [corresponding to the fcc(111) lattice face of a bulk C60 crystal], where interstitial sites are not considered. Each site corresponds to a unit cell with area $A = 1a \times 0.866a$ where a is the lattice constant. With this setup, we effectively halve the number of potential valleys within each plane, therefore each simulated diffusion step reflects two movements between energetic minima. In the experiments of Ganapathy *et al.* [23] the parameter d for the step-edge diffusion in a colloidal system is given as $d = 2.8$. Due to our coarse graining, we here choose $d = 1.4$ (as discussed in more detail
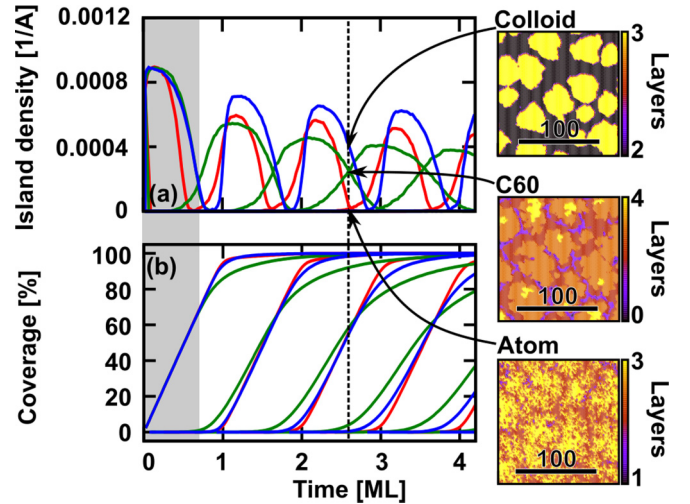

FIG. 2. Part (a) depicts the island density $\rho_{\text{n}}(t)$ related to layer n (in units of the area $A = 0.866a^2$ of one unit cell with lattice constant a) for atomic, C60, and colloidal growth, while part (b) depicts the layer coverage $\Theta_{\text{n}}(t)$. Time is measured relative to the time of the formation of one monolayer (ML). The gray block depicts the region in which $\Theta_{\text{n}}(t)$ evolves identically for all three systems, while the dashed line marks the time related to the snapshots (right). The length bars indicate 100 lattice constants.

in Ref. [18]). In most of the simulations we use a surface of 1000×1000 lattice sites.

We characterize the surface growth in terms of three observables. The first (in-plane) observable is the island density $\rho_{\text{n}}(t) = N_{\text{n}}^{\text{islands}}(t)/N^{\text{sites}}$, where $N_{\text{n}}^{\text{islands}}$ and N^{sites} are the number of islands in the nth layer and the number of simulated lattice sites, respectively. Second, the out-of-plane growth is studied via the layer coverage $\Theta_{\text{n}}(t) = N_{\text{n}}^{\text{particles}}(t)/N^{\text{sites}}$, where $N_{\text{n}}^{\text{particles}}(t)$ denotes the number of particles in the nth layer (i.e., number of occupied sites). Third, to quantify the average size and morphology of islands, we calculate the radius of gyration (averaged over all islands j), $R_{\text{gyr}}(t) = \sum_j R_{\text{gyr},j}(t)/N^{\text{islands}}$. The gyration radius of island j is defined as $R_{\text{gyr},j}(t) = \sqrt{\sum_{i \in j} (\mathbf{x}_i - \bar{\mathbf{x}}_j)^2 / N^{i \in j}}$, where $\mathbf{x} = (x,y)$ and $N^{i \in j}$ is the number of particles i in island j. By definition, $R_{\text{gyr},j}(t)$ gives the average distance of particles i in the island j from the center of mass ($\bar{\mathbf{x}}_j$), so it is larger for a dendritic island than for a compact island with the same number of particles.

Numerical results for $\rho_{\text{n}}(t)$ and $\Theta_{\text{n}}(t)$ are depicted in Figs. 2(a) and 2(b). The oscillations in $\rho_{\text{n}}(t)$ reflect the nucleation and subsequent merging of islands during the growth of each monolayer, while the periodic increases in $\Theta_{\text{n}}(t)$ describe the filling of individual layers. For obtaining the data in Fig. 2, we have scaled the temperatures such that the coverage and island density during growth of the first layer, i.e., in the range of time where in-plane diffusion processes dominate, match as well as possible. Specifically, $T^{\text{atom}} = 77\,^{\circ}\text{C}$, $T^{\text{C60}} = 40\,^{\circ}\text{C}$, and $T^{\text{colloid}} = 28.5\,^{\circ}\text{C}$. This sequence of temperatures corresponds to the sequence of the neighbor energies E_{n} (see above). Despite this optimized temperature scaling we find small differences during the early
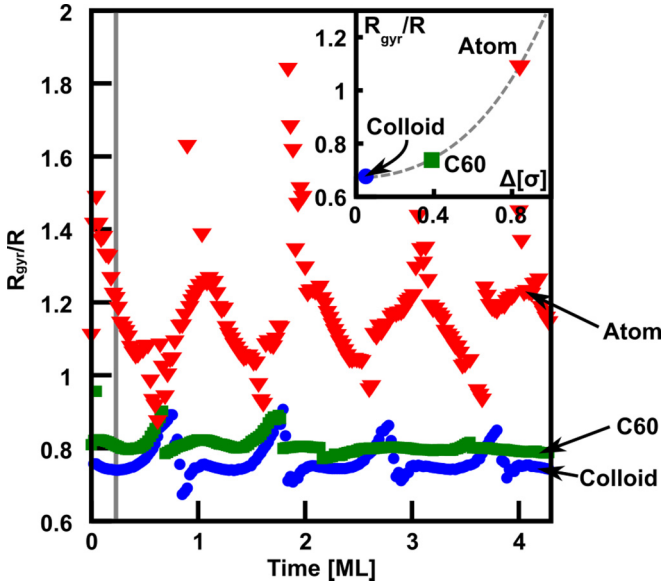
FIG. 3. The normalized gyration radius R_{gyr}/R as a function of time [38]. Each data point corresponds to the maximum of the data of different layers n. The gray vertical line indicates the time related to the inset, where R_{gyr}/R is plotted as a function of the attraction range Δ (the gray dashed line is a guide to the eye). For the colloidal system, $\Delta = 0.05$. For C60 and the atomic system, Δ has been chosen as the distance where the attractive part of $V(r)$ has dropped to 10% of the maximal attraction.

stages of growth, as visible, e.g., in the time dependence of $\rho_{\mathrm{n}}(t)$ of atoms as compared to C60 and colloids [see Fig. 2(a)]. These differences are essentially a consequence of the fact that the binding energies [E_{n} in Eq. (1)] relative to the barrier associated to free diffusion (E_{free}) are much smaller in C60 (and in colloids) than in atoms, reflecting that Δ_{C60} and $\Delta_{\mathrm{colloid}} < \Delta_{\mathrm{atom}}$ [18]. These details of in-plane hopping are indeed expected to strongly influence the in-plane morphology.

Further important information on the in-plane island formation is revealed by the radius of gyration R_{gyr} plotted in Fig. 3. Specifically, we consider the ratio $R_{\mathrm{gyr}}(t)/R$ where R is the average of island radii $R_j = \sqrt{N^{i \in j} A/\pi}$ [38]. Thus, R_{gyr}/R is a measure of inverse compactness. As seen from Fig. 3, the three systems indeed display significant differences from the very onset of growth, i.e., already in the submonolayer. The most pronounced time dependence and the largest amplitudes of R_{gyr}/R versus t occur in the atomic system. In fact, for small times we find a monotonous dependency of the ratio R_{gyr}/R on the attraction range Δ (see inset of Fig. 3), a trend which is preserved during the later stages of multilayer growth. This implies that atoms (having the largest Δ) tend to nucleate into much more fractal (less compact) islands than C60 and colloids (for the temperature scaling applied above). We can see this trend also in the snapshots in Fig. 2.

Discussion. We now come back to the question of scalability. As shown in Fig. 2, both the island density and layer coverages appear to be essentially scalable during the growth

of the first ML. However, already at this stage the systems deviate in their island morphology (see Fig. 3). As soon as the second layer nucleates, all three systems deviate significantly in all observables. This can easily be seen in the snapshots taken after 2.6 ML in Fig. 2.

The attraction range Δ enters essentially all aspects of growth by impacting the effective diffusion barrier in plane and out of plane. While there is certainly a complex interplay of various parameters, the following rather general trends can be identified. Within each layer, islands merge the earlier the larger Δ [see positions of the minima in $\rho_{\mathrm{n}}(t)$ in Fig. 2]. Further, Δ influences the degree of fractality at a given time: For the smallest Δ (which we have realized by colloids), we observe the most compact islands (see Fig. 3).

To conclude, our work provides strong evidence that key aspects of growth, particularly the out-of-plane structure formation following the first ML, do *not* simply scale with the size of the particles, even after scaling of the temperature. A major ingredient for the observed limitations of scaling of, e.g., the time-dependent layer coverage $\Theta_{\mathrm{n}}(t)$, is that the *range* Δ of typical attractive interactions relative to the particle diameter markedly decreases when going from atoms to C60 to colloids. As a consequence, the entire potential landscape experienced by a tracer particle changes, and so do the diffusion barriers. This concerns, in particular, the effective step-edge (Ehrlich-Schwoebel) barrier. Moreover, for colloids with very short-ranged (depletion) interactions the step-edge barrier can even change its origin from energetic (such as in atoms) to purely geometric.

Thus, "size scaling" by adjusting the temperature is generally possible only to a limited extent for submonolayer growth. The corresponding out-of-plane behavior deviates substantially. This central conclusion is not dependent on the fine details of the potentials but rather a generic consequence of the different interaction ranges Δ. The case that, in colloidal systems, $V(r)$ can be perfectly tuned (by surface functionalization, adjusting electrostatics, etc.) such that after size scaling it matches that of atoms and the growth behavior is similar, appears rather hypothetical (although in principle possible). Moreover, due to the different nature of the step-edge barriers between atoms and molecules, on the one hand, and colloids, on the other hand, we speculate that also the temperature dependence of the growth will generally differ.

Therefore, while experiments for atomic systems and established growth theories indicate the possible scenarios, the resulting morphologies can strictly not be scaled in size to quantitatively obtain those for larger particles. On a more general level, the results relate to fundamental work on the impact of Δ on the equilibrium phase behavior [39], which changes ultimately if the interaction range is changed, leading eventually to the absence of a liquid phase for certain short-ranged systems. In this sense, the present findings are the nonequilibrium growth analog to the impact of Δ on the equilibrium phase diagram.

[1] T. Michely and J. Krug, *Islands, Mounds and Atoms* (Springer, Berlin, Heidelberg, 2004).

[2] A. Pimpinelli and J. Villain, *Physics of Crystal Growth* (Cambridge University Press, Cambridge, 1989).

[3] B. Freedman, G. Bartal, M. Segev, R. Lifshitz, D. Christodoulides, and J. Fleischer, Nature (London) **440**, 1166 (2006).

[4] G. Hlawacek, P. Puschnig, P. Frank, A. Winkler, C. Ambrosch-Draxl, and C. Teichert, Science **321**, 108 (2008).

[5] M. Sparenberg, A. Zykov, P. Beyer, L. Pithan, C. Weber, Y. Garmshausen, F. Carla, S. Hecht, S. Blumstengel, F. Henneberger, and S. Kowarik, Phys. Chem. Chem. Phys. **16**, 26084 (2014).

[6] J. V. Barth, G. Costantini, and K. Kern, Nature (London) **437**, 671 (2005).

[7] J. R. Savage, S. F. Hopp, R. Ganapathy, S. J. Gerbode, A. Heuer, and I. Cohen, Proc. Natl. Acad. Sci. USA **110**, 9301 (2013).

[8] C. P. Joshi, Y. Shim, T. P. Bigioni, and J. G. Amar, Phys. Rev. E **90**, 032406 (2014).

[9] L. Xu, W. Ma, L. Wang, C. Xu, H. Kuang, and N. A. Kotov, Chem. Soc. Rev. **42**, 3114 (2013).

[10] V. N. Manoharan, Science **349**, 1253751 (2015).

[11] M. Einax, W. Dieterich, and P. Maass, Rev. Mod. Phys. **85**, 921 (2013).

[12] M. F. Gyure, J. J. Zinck, C. Ratsch, and D. D. Vvedensky, Phys. Rev. Lett. **81**, 4931 (1998).

[13] H. Brune, K. Bromann, H. Röder, K. Kern, J. Jacobsen, P. Stoltze, K. Jacobsen, and J. Nørskov, Phys. Rev. B **52**, R14380 (1995).

[14] H. Brune, Surf. Sci. Rep. **31**, 125 (1998).

[15] J. W. Evans, P. A. Thiel, and M. C. Bartelt, Surf. Sci. Rep. **61**, 1 (2006).

[16] J. Krug, Adv. Phys. **46**, 139 (1997).

[17] S. Kowarik, A. Gerlach, S. Sellner, F. Schreiber, L. Cavalcanti, and O. Konovalov, Phys. Rev. Lett. **96**, 125504 (2006).

[18] S. Bommel, N. Kleppmann, C. Weber, H. Spranger, P. Schaefer, J. Novak, S. V. Roth, F. Schreiber, S. H. L. Klapp, and S. Kowarik, Nat. Commun. **5**, 5388 (2014).

[19] J. E. Goose, E. L. First, and P. Clancy, Phys. Rev. B **81**, 205310 (2010).

[20] W. C. Wang, D. Y. Zhong, J. Zhu, F. Kalischewski, R. F. Dou, K. Wedeking, Y. Wang, A. Heuer, H. Fuchs, G. Erker, and L. F. Chi, Phys. Rev. Lett. **98**, 225504 (2007).

[21] P. K. Jana and A. Heuer, J. Chem. Phys. **138**, 124708 (2013).

[22] N. Kleppmann and S. H. L. Klapp, Phys. Rev. B **91**, 045436 (2015).

[23] R. Ganapathy, M. R. Buckley, S. J. Gerbode, and I. Cohen, Science **327**, 445 (2010); T. L. Einstein and T. J. Stasevich, *ibid.* **327**, 423 (2010).

[24] G. Ehrlich and F. G. Hudda, J. Chem. Phys. **44**, 1039 (1966).

[25] R. L. Schwoebel, J. Appl. Phys. **40**, 614 (1969).

[26] F. Schreiber, Phys. Status Solidi A **201**, 1037 (2004).

[27] J. E. Jones, Proc. R. Soc. London, Ser. A **106**, 463 (1924).

[28] S. Asakura and F. Oosawa, J. Chem. Phys. **22**, 1255 (1954).

[29] L. A. Girifalco, J. Phys. Chem. **96**, 858 (1992).

[30] S. P. Tewari, G. Dhingra, and P. Silotia, Int. J. Mod. Phys. B **24**, 4281 (2010).

[31] P. Bryk, R. Roth, M. Schoen, and S. Dietrich, Europhys. Lett. **63**, 233 (2003).

[32] M. Holfes-Cerfon, Steven J. Gortler, and M. P. Brenner, Proc. Natl. Acad. Sci. USA **110**, E5 (2013).

[33] A. K. Jones, A. Ballestad, T. Li, M. Whitwick, J. Röttler, and T. Tiedje, Phys. Rev. B **79**, 205419 (2009).

[34] I. K. Marmorkos and S. Das Sarma, Phys. Rev. B **45**, 11262 (1992).

[35] S. Clarke and D. D. Vvedensky, J. Appl. Phys. **63**, 2272 (1988).

[36] T. J. Oliveira and F. D. A. Aarão Reis, Phys. Rev. B **87**, 235430 (2013).

[37] This *ansatz* has a specific effect on the degree of fractality, but this is not crucial for the nucleation density [as can also be seen in Fig. 2(b)]. However, the *ansatz* does not impact our overall conclusions concerning the scalability.

[38] Note that for the idealized case of a circular disk with homogeneous particle distribution, $R_{\mathrm{gyr}}/R = \sqrt{1/2}$. Smaller values can occur in the case of islands of very few particles, where the discrete nature of the particle distribution becomes relevant. We also note that one data point in Fig. 3 has been omitted due to overlap with the inset.

[39] M. H. J. Hagen, E. J. Meijer, G. C. A. M. Mooij, D. Frenkel, and H. N. W. Lekkerkerker, Nature (London) **365**, 425 (1993).